

# Anderson localization of partially incoherent light

---

Čapeta, Davor; Radić, Juraj; Szameit, Alex; Segev, Mordechai; Buljan, Hrvoje

Source / Izvornik: **Physical Review A, 2011, 84**

**Journal article, Published version**

**Rad u časopisu, Objavljena verzija rada (izdavačev PDF)**

<https://doi.org/10.1103/PhysRevA.84.011801>

Permanent link / Trajna poveznica: <https://um.nsk.hr/um:nbn:hr:217:203371>

Rights / Prava: [In copyright](#)/[Zaštićeno autorskim pravom.](#)

Download date / Datum preuzimanja: **2025-01-01**



Repository / Repozitorij:

[Repository of the Faculty of Science - University of Zagreb](#)



## Anderson localization of partially incoherent light

D. Čapeta,<sup>1</sup> J. Radić,<sup>1</sup> A. Szameit,<sup>2</sup> M. Segev,<sup>2</sup> and H. Buljan<sup>1</sup>

<sup>1</sup>*Department of Physics, University of Zagreb, PP 332, 10000 Zagreb, Croatia*

<sup>2</sup>*Physics Department and Solid State Institute, Technion, Haifa 32000, Israel*

(Received 16 February 2011; published 11 July 2011)

We study Anderson localization and propagation of partially spatially incoherent wavepackets in linear disordered potentials, motivated by the insight that interference phenomena resulting from multiple scattering are affected by the coherence of the waves. We find that localization is delayed by incoherence: the more incoherent the waves are, the longer they diffusively spread while propagating in the medium. However, if all the eigenmodes of the system are exponentially localized (as in one- and two-dimensional disordered systems), any partially incoherent wavepacket eventually exhibits localization with exponentially decaying tails, after sufficiently long propagation distances. Interestingly, we find that the asymptotic behavior of the incoherent beam is similar to that of a single instantaneous coherent realization of the beam.

DOI: [10.1103/PhysRevA.84.011801](https://doi.org/10.1103/PhysRevA.84.011801)

PACS number(s): 42.25.Dd, 42.25.Kb, 72.15.Rn

The phenomenon of Anderson localization was conceived in the context of disordered electronic systems [1]; however, localization phenomena have been extensively studied also in other systems [2–17] including optics [2,3,5–14] and ultracold quantum gases [15–17]. For a direct observation of the phenomena, optical and ultracold atomic systems have some profound advantages over the condensed matter systems: the influence of the environment such as thermal fluctuations and phonons can be minimized to become negligible, and nonlinearity or interactions can be controlled and virtually turned off. Nonlinearity in optics can be controlled by the intensity of light, whereas interactions of ultracold gases can be tuned via Feshbach resonances. In contrast, electron-electron and electron-phonon interactions are always present in condensed matter systems. These influences are important since they affect interference, and Anderson localization arises from interference among multiple scattering events from disorder in the medium.

Here we address Anderson localization of waves with imperfect coherence. We ask whether an initial finite-size partially incoherent wavepacket would spread through a linear disordered potential or would its spreading be stopped by virtue of disorder? We demonstrate our findings on an optical  $(1 + 1)$ D potential and discuss their implications to other wave systems. A superficial answer to the question above may be that, since incoherence destroys interference effects, a sufficiently incoherent wavepacket will diffuse through the random medium without ever being localized. However, an incoherent wave can be thought of as a superposition of coherent modes with stochastically varying coefficients [18]. Each coherent mode is expected to undergo localization, hence the entire wavepacket should localize. Our study reveals that coherence indeed affects the properties of evolving wavepackets, in a sense that more incoherent beams spread more while propagating through the random medium. However, if the system's eigenmodes are all localized, as is the case for all one-dimensional  $[(1 + 1)$ D] and two-dimensional  $[(2 + 1)$ D] fully disordered systems [19], the incoherent wavepacket will eventually become Anderson localized. Finally, we find that a typical instantaneous coherent speckled realization of the

incoherent beam exhibits the same asymptotic behavior as the time-averaged incoherent wavepacket.

The idea that localization could be observed in optics dates back to the beginning of the 1980s [2,3]. The experiments on so-called weak localization [4], which can be pictured in terms of a coherent backscattering process, were soon to follow [5,6]. Experiments on strong localization in random media were performed in various systems [8–10]. In 1989, a nontraditional idea for observing localization was proposed: the transverse localization scheme [7], which exploits the equivalence between the Schrödinger equation and the paraxial wave equation for light. Indeed, this scheme was used for a clear demonstration of Anderson localization in random optical lattices [11], for the observation of Anderson modes [12], and localization near an interface [13]. All of these have dealt with fully coherent waves only. In a different domain, the propagation of partially incoherent light in random media is a subject of considerable interest (e.g., see [20]). However, in the context of localization, the only studies on incoherent light were on enhanced backscattering [21,22], which is considered a precursor to Anderson localization. To the best of our knowledge, strong localization with partially incoherent light has never been studied.

Consider the propagation of a partially spatially incoherent optical beam, linearly polarized, originating from a quasi-monochromatic continuous-wave source. Such a beam can be constructed by sending a laser beam through a rotating diffuser (e.g., see [23]). Its state at a given propagation distance  $z$  can be described in terms of the mutual coherence function [18],  $B(x_1, x_2, z) = \langle E^*(x_2, z, t)E(x_1, z, t) \rangle_t$ , where  $\langle \dots \rangle_t$  is the time-average, and  $E$  is the stochastic field. Instead of  $B(x_1, x_2, z)$ , the state of the system can be described by an orthonormal set of modes  $\psi_j(x, z)$  ( $j = 1, 2, \dots$ ), and their modal weights  $\lambda_j$ , which are obtained from the eigenvalue equation [18]:  $\int dx_2 B(x_1, x_2, z) \psi_j(x_2, z) = \lambda_j \psi_j(x_1, z)$ ; i.e.,  $B(x_1, x_2, z) = \sum_j \lambda_j \psi_j^*(x_2, z) \psi_j(x_1, z)$ .

We analyze linear propagation of such a beam in the transverse localization scheme [7], in a waveguide array defined by the index of refraction  $n_{\text{index}}^2 = n_0^2 + 2n_0 \delta n(x)$ , where  $n_0$  is a constant term, while  $\delta n(x)$  describes disorder.

The propagation of the beam along the  $z$  axis is governed by the Schrödinger equation [11],

$$i \frac{\partial \psi}{\partial z} = -\frac{1}{2k} \frac{\partial^2 \psi}{\partial x^2} - \frac{\delta n(x)k}{n_0} \psi, \quad (1)$$

where  $k = n_0\omega/c$  is the wave vector,  $\omega$  is the temporal frequency of the beam carrier, and  $c$  is the speed of light.

In our simulations, we analyze the evolution of Gaussian input beams:  $B(x_1, x_2, 0) = I_0 \exp[-(x_1 + x_2)^2/4\sigma_I^2 - (x_1 - x_2)^2/\sigma_C^2]$ , where  $\sigma_I$  and  $\sigma_C$  are the spatial and the coherence widths of the beam, respectively. In disordered media, the propagation depends on the particular realization of the random potential  $\delta n(x)$ . Hence, we calculate the mutual coherence for many realizations of the disorder to find the disorder ensemble average [11]:  $\langle B(x_1, x_2, z) \rangle_d$ .

The disordered potential used in our simulations is illustrated in Fig. 1(a). The index of refraction varies randomly (with uniform distribution) between  $\delta n = 0$  and  $\delta n = 1.2 \times 10^{-3}$ . The width of every rectangular potential unit shown in Fig. 1(a) is  $2.7 \mu\text{m}$ , but their mutual distances are random: first we fix the leftmost rectangle in its position, and then add the adjacent ones to the right such that their distance (center to center) is between 5 and  $9 \mu\text{m}$  (chosen at random), and so on. Such a disordered medium can be created experimentally by using the ultrafast direct laser-writing technique [13].

Because the system is linear, the dynamics is described in terms of the modes of the system  $u_n$  and their propagation constants  $\beta_n$ , which obey

$$\beta_n u_n = \frac{1}{2k} u_n''(x) + \frac{\delta n(x)k}{n_0} u_n, \quad n = 1, 2, \dots \quad (2)$$

The  $\beta_n$ s are arranged in decreasing order (equivalent to increasing order of energies in quantum systems). Every initial coherent wave  $\psi_j(x, 0)$  is projected onto the system's

modes  $u_n$ :  $c_{j,n} = \int dx \psi_j(x, 0) u_n^*(x)$ , yielding  $\psi_j(x, z) = \sum_n c_{j,n} u_n(x) e^{i\beta_n z}$ , that is,

$$B(x_1, x_2, z) = \sum_{j,n,m} \lambda_j c_{j,n}^* c_{j,m} u_n^*(x_2) u_m(x_1) e^{i(\beta_m - \beta_n)z}. \quad (3)$$

It is reasonable to conjecture that after sufficiently long propagation  $z$ , the mutual coherence is approximately

$$B(x_1, x_2, z \rightarrow \infty) = \sum_{j,n} \lambda_j |c_{j,n}|^2 u_n^*(x_2) u_n(x_1). \quad (4)$$

From Eqs. (3) and (4), we clearly see that if the medium is infinitely broad and the potential is fully random, then, since all the eigenmodes  $u_n$  are Anderson localized, any initial finite-width partially incoherent beam will not diffuse during propagation despite its incoherence. One can expect that, after sufficiently long propagation, the tails of the incoherent beam will become exponentially decaying:  $B(x, x, z \rightarrow \infty) \propto \exp(-\gamma|x|)$ , with  $\gamma$  corresponding to the excited eigenmode  $u_n$ , which has the slowest decay. However, in reality, all samples have finite transverse ( $L$ ) and longitudinal ( $Z$ ) size; hence, we explore the finite-size effects.

First we calculate the eigenvectors/eigenvalues of the potential  $\delta n(x)$ . We use the LAPACK implementation of the MRRR algorithm [24], with Dirichlet boundary conditions  $u_n = 0$  at  $x = \pm L/2$ . Typical eigenfunctions are shown in Figs. 1(b)–1(d). Up to some critical value of  $n$ , the spatial extent of the eigenfunctions  $u_n$  is smaller than  $L$  [see Fig. 1(b)], whereas above this value they extend to one or both of the boundaries [see Fig. 1(c)]. From Fig. 1(d), we see that the amplitude of localized  $u_n(x)$  decays exponentially,  $\log |u_n(x)| \propto \exp(\gamma_n x)$ , which is a fingerprint of Anderson localization. From these eigenmodes, we calculate their Lyapunov exponents as follows: We form a set  $\{|u_n(x_{\max})|\}$  of local maxima of  $|u_n(x)|$ , and then fit  $-\gamma_n |x - x_c| + b$  to the set of points  $\log |u_n(x_{\max})|$ , to obtain  $\gamma_n$  for every  $u_n$ . For the lowest eigenstates with too few local extrema,  $|u_n|$  was fitted. The Lyapunov exponents, averaged over 40 different realizations of the random potential, are shown in Fig. 2(a) as a function of  $n$ ; the standard deviation is as small as the thickness of the line implying the self-averaging property of the exponents. A different calculation of Lyapunov exponents via the transfer matrix approach [19] (for an essentially infinite

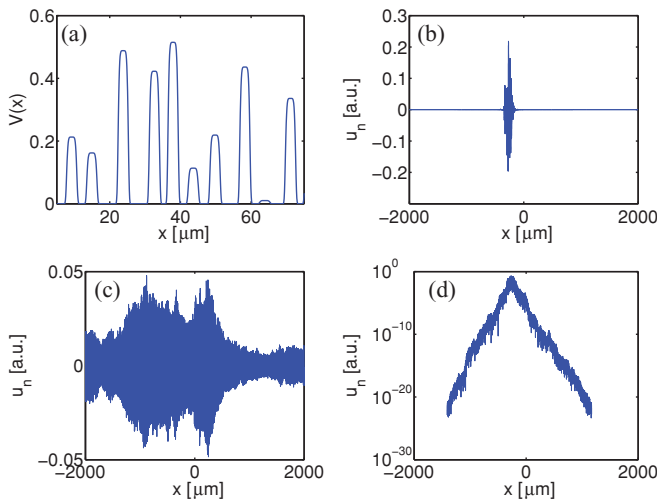


FIG. 1. (Color online) The disordered potential and its eigenmodes. (a) Small section of the dimensionless disordered potential  $V(x) = -2\delta n(x)(kx_0)^2/n_0$ , where  $k = 2\pi n_0/\lambda$ ,  $\lambda = 514 \text{ nm}$ ,  $x_0 = 1 \mu\text{m}$ ,  $n_0 = 1.45$ . (b, c) Typical eigenfunctions of the structure with a smaller (b) and larger (c) spatial extent, in a sample of width  $L = 4 \text{ mm}$ . (d) Logarithmic plot of  $|u_n(x)|$  from (b) with exponentially decaying tails, which are the fingerprint of Anderson localization.

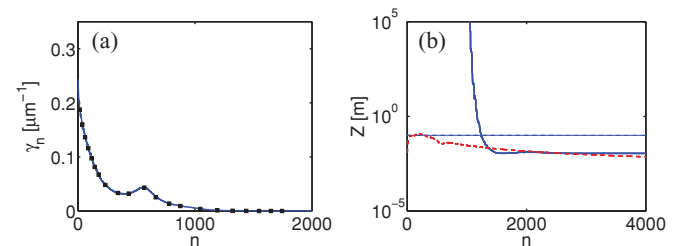


FIG. 2. (Color online) (a) Lyapunov exponents  $\gamma_n$  extracted from the eigenfunctions  $u_n$  (solid blue line) and via the transfer matrix approach (black squares). Shown are averages over 40 different realizations of the random potential; the standard deviation is smaller than the thickness of the line. (b) The Thouless (solid blue line) and the Heisenberg (dashed red line) times (propagation distances) vs.  $n$  for the system with  $L = 4 \text{ mm}$ . Horizontal line depicts  $Z = 10 \text{ cm}$ . See text for details.

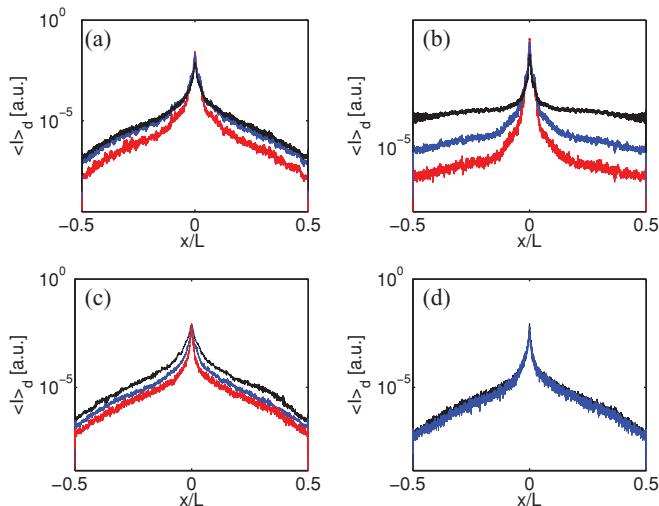


FIG. 3. (Color online) Intensities of the incoherent beam after  $Z = 10$  cm of propagation, for different system parameters, averaged over 40 realizations of the disorder. (a,b) Beam intensity for absorbing (a) and reflecting (b) boundary conditions for beams with  $\sigma_I = 10 \mu\text{m}$ , and  $\sigma_C = 1 \mu\text{m}$  (top black line),  $3 \mu\text{m}$  (middle blue line), and  $5 \mu\text{m}$  (bottom red line);  $L = 4$  mm. (c) Beam intensity for absorbing boundary conditions and three values of  $L$ : 2, 4, and 8 mm (top to bottom) [ $\sigma_I = 10 \mu\text{m}$ ,  $\sigma_C = 1 \mu\text{m}$ ]. (d) The intensity for one specific instantaneous initial realization of the incoherent field (lower blue line) and the time-averaged intensity (upper black line) [ $\sigma_I = 10 \mu\text{m}$ ,  $\sigma_C = 1 \mu\text{m}$ ,  $L = 8$  mm, absorbing boundary conditions].

sample), displayed as black squares in Fig. 2(a), underpins our results. The overall trend is such that the Lyapunov exponents decrease with increasing  $n$  (decreasing  $\beta_n$ ), except for a small hump, which is a consequence of relatively small fluctuations in distances between adjacent potential peaks [Fig. 1(a)] (if we allow larger fluctuations the hump disappears).

In an experiment with finite-size samples, a partially incoherent initial wavepacket is likely to excite both modes that are Anderson localized on a scale smaller than  $L$  and modes extending to the boundary. To investigate the finite-size effects, we numerically evolve the wavepacket with absorbing boundary conditions [Fig. 3(a)], and then with reflecting boundary conditions [Fig. 3(b)]. In experiments, reflecting boundary conditions can be obtained via total internal reflection, and absorbing boundary conditions can be obtained by placing a properly designed layer of highly absorbing material on the sample edges. The initial size of the beam is  $\sigma_I = 10 \mu\text{m}$ , and the degree of coherence varies:  $\sigma_C = 1, 3$ , and  $5 \mu\text{m}$ ;  $L = 4$  mm. Reflecting boundary conditions are taken into account by using Eq. (3) with  $u_n$  obeying Dirichlet boundary conditions. Absorbing boundary conditions are included as an imaginary index of refraction,  $\text{Im} \delta n_{\text{abs}} > 0$ , present *only* close to the boundaries:  $\delta n_{\text{abs}} = 0$  for  $|x| < 0.96 \frac{L}{2}$ .

From the simulations with absorbing edges we find that, after sufficiently long propagation, the intensity structure has exponentially decaying tails:  $\langle I \rangle_d \propto \exp(-\gamma|x|)$ . All graphs have approximately the same value for the slope,  $\gamma = 3.2 \times 10^{-3} \mu\text{m}^{-1}$ . This is in accordance with our analysis of eigenstates. The part of the beam exciting eigenstates that touch (or are in the very vicinity of) the edges gets absorbed during propagation. The remaining part excites only

exponentially decaying eigenstates, which yields the intensity plotted in Fig. 3(a). The value of  $\gamma$  found from graphs in Fig. 3(a) correspond to the slowest decay rate  $\gamma_n$  of the eigenstate  $u_n$ , which is excited and which does not overlap with the absorbing boundary, i.e.,  $\langle u_n | \delta n_{\text{abs}}(x) | u_n \rangle \approx 0$  (one should take into account a factor 2 because  $I = \langle |E|^2 \rangle_t$ ).

Next we consider the Thouless ( $Z_T$ ) and Heisenberg ( $Z_H$ ) times (propagation distances) in our system. The former tells us the average time it takes for a particle to diffuse across the sample, and the latter is the longest time the particle can travel inside the sample without visiting the same region twice (e.g., see [14]). In our case,  $Z_T$  corresponds to the inverse linewidth ( $1/\Delta\beta_n$ ) of the eigenstates with absorbing boundary conditions. In calculating  $Z_T(n)$ , we have averaged  $1/\Delta\beta_n$  over 20 adjacent eigenstates and then over 40 realizations of the potential. In the same fashion, we have calculated the average inverse level spacing, which yields  $Z_H(n)$ . Figure 2(b) shows  $Z_T$  and  $Z_H$  vs.  $n$ . Evidently the Thouless time is effectively infinite for  $n < 1200$ , indicating Anderson localization in our finite sample, whereas for greater  $n$  values the two times are on comparable scales.

From Fig. 3(a) we conclude that the more coherent the light is, the stronger the localization effect is, in a sense that less power is absorbed by the walls. The slope  $\gamma$  is identical for every  $\sigma_C$ , because in every case the highest of the localized modes was excited. It is interesting to note that the values  $\gamma$  obtained after transport simulations (expansion) *depend* on the size of the sample  $L$  and scale approximately as  $\gamma \propto L^{-1}$ . We checked this trend for  $L = 2, 4$ , and  $8$  mm; see Fig. 3(c). The observed scaling is found to be in agreement with Ref. [25], where it was shown that the logarithm of the dimensionless resistance scales as the length in case of localization.

Figure 4 shows a typical change in the spatial power spectrum for propagation with different boundary conditions. In the case of absorbing edges, there is a clear cutoff in  $k$  space, indicating that the modes  $u_n$  composed of plane waves with  $k$  values above the cutoff spread to the absorbing boundaries. Such absorption increases the spatial coherence of the beam. For reflecting boundary conditions, the final spectrum has the same shape as the initial spectrum, with fluctuations on top of the average.

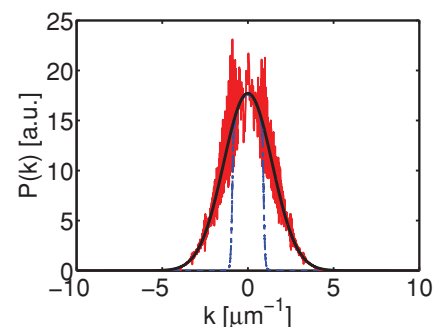


FIG. 4. (Color online) Spatial power spectrum of the incoherent beam after  $Z = 10$  cm of propagation in a disordered medium with absorbing (thin dashed blue line) and reflecting (solid red line) edges, for an initial beam (thick solid black line) defined by  $\sigma_I = 10 \mu\text{m}$ ,  $\sigma_C = 1 \mu\text{m}$ . All plots are averages over 40 realizations of the disorder.

A partially spatially incoherent (quasimonochromatic) beam can be thought of as a train of fully coherent fields with intricate field structures, which are replaced on a time scale  $\sim \Delta t_c$  (the temporal coherence time); quasimonochromatic means that  $\Delta t_c \gg Z/c$ . In experiments, one instantaneous realization of the incoherent field is obtained by stopping the diffuser [23]. Interestingly, we find that one instantaneous field realization will asymptotically have exponentially decaying tails similar to those of the time-averaged intensity [see Fig. 3(d)]. The asymptotic intensity evidently depends both on the degree of coherence and the spatial structure of the input field.

We can extend our conclusions to hold for spatially and temporally incoherent beams of light ( $\Delta t_c < Z/c$ ), such as the one made from an incandescent light bulb in Ref. [26]. In this case, a space-time mutual coherence function describing the beam can be transformed into the space-frequency domain [18,27]. Because our results hold for every frequency component separately (with different numerical values for different frequencies), due to linear superposition, they also hold for the whole beam.

In conclusion, we have predicted the properties of Anderson localization of partially spatially incoherent beams in disordered linear (1 + 1)D photonic structures. We conclude that more incoherent light will diffusively spread more through the

random medium than coherent light; however, the incoherent wavepacket will display exponentially decaying tails after sufficiently long propagation. We have discussed the finite-size effects and extended our conclusions for spatially and temporally incoherent light beams. Finally, we note that our results correspond to partially condensed *noninteracting* Bose-Einstein condensates (BECs) in 1D disordered potentials, the strongly interacting 1D Bose gases [28], and noninteracting 1D Fermi gases [29]. To mimic partially condensed interacting BECs [30], one should include nonlinearity, which we leave for further studies.

*Note added in proof.* Recently, related work [31] appeared on the arXiv, suggesting that in some disordered potentials Lyapunov exponents can increase with the increase of energy (in some interval). This is exactly the phenomenon observed in our Fig. 2(a): The small bump therein. In this Rapid Communication, we have shown that this effect exists in a classical wave system.

This work was supported in part by the Croatian-Israeli scientific cooperation program. A.S. thanks the Leopoldina—The German Academy of Science (Grant No. LPDS 2009-13), and H.B. thanks the MZOS (Grant No. 119-0000000-1015) and the Croatian National Foundation for Science.

- 
- [1] P. W. Anderson, *Phys. Rev.* **109**, 1492 (1958).  
 [2] S. John, *Phys. Rev. Lett.* **53**, 2169 (1984).  
 [3] P. W. Anderson, *Philos. Mag. B* **52**, 505 (1985).  
 [4] E. Akkermans, R. Maynard, *J. Phys. Lett.* **46**, 1045 (1985).  
 [5] M. P. Van Albada and A. Lagendijk, *Phys. Rev. Lett.* **55**, 2692 (1985).  
 [6] P.-E. Wolf and G. Maret, *Phys. Rev. Lett.* **55**, 2696 (1985).  
 [7] H. De Raedt, A. Lagendijk, and P. de Vries, *Phys. Rev. Lett.* **62**, 47 (1989).  
 [8] D. S. Wiersma, P. Bartolini, A. Lagendijk, and R. Righini, *Nature (London)* **390**, 671 (1997).  
 [9] A. A. Chabanov, M. Stoytchev, and A. Z. Genack, *Nature (London)* **404**, 850 (2000).  
 [10] M. Störzer, P. Gross, C. M. Aegerter, and G. Maret, *Phys. Rev. Lett.* **96**, 063904 (2006).  
 [11] T. Schwartz, G. Bartal, S. Fishman, and M. Segev, *Nature (London)* **446**, 52 (2007).  
 [12] Y. Lahini *et al.*, *Phys. Rev. Lett.* **100**, 013906 (2008).  
 [13] A. Szameit *et al.*, *Opt. Lett.* **35**, 1172 (2010).  
 [14] A. Lagendijk, B. van Tiggelen, and D. S. Wiersma, *Physics Today*, August 2009, page 24.  
 [15] J. Billy *et al.*, *Nature (London)* **453**, 891 (2008).  
 [16] G. Roati *et al.*, *Nature (London)* **453**, 895 (2008).  
 [17] For a recent review see L. Sanchez-Palencia and M. Lewenstein, *Nature Phys.* **6**, 87 (2010).  
 [18] L. Mandel and E. Wolf, *Optical Coherence and Quantum Optics* (Cambridge Press, New York, 1995).  
 [19] E. N. Economou, *Green's Functions in Quantum Physics* (Springer, Berlin, 2006).  
 [20] G. Gbur and E. Wolf, *J. Opt. Soc. Am. A* **19**, 1592 (2002).  
 [21] A. Wax, S. Bali, and J. E. Thomas, *Phys. Rev. Lett.* **85**, 66 (2000).  
 [22] Y. L. Kim *et al.*, *Opt. Lett.* **29**, 1906 (2004).  
 [23] M. Mitchell, Z. Chen, M. F. Shih, and M. Segev, *Phys. Rev. Lett.* **77**, 490 (1996).  
 [24] Inderjit S. Dhillon, Ph.D. thesis, EECS Department, University of California, Berkeley (1997).  
 [25] P. W. Anderson, D. J. Thouless, E. Abrahams, and D. S. Fisher, *Phys. Rev. B* **22**, 3519 (1980).  
 [26] M. Mitchell and M. Segev, *Nature (London)* **387**, 880 (1997).  
 [27] H. Buljan, A. Šiber, M. Soljačić, and M. Segev, *Phys. Rev. E* **66**, 035601 (2002).  
 [28] J. Radić, V. Bačić, D. Jukić, M. Segev, and H. Buljan, *Phys. Rev. A* **81**, 063639 (2010).  
 [29] H. Buljan, O. Manela, R. Pezer, A. Vardi, and M. Segev, *Phys. Rev. A* **74**, 043610 (2006).  
 [30] H. Buljan, M. Segev, and A. Vardi, *Phys. Rev. Lett.* **95**, 180401 (2005).  
 [31] M. Piraud, A. Aspect, and L. Sanchez-Palencia, e-print arXiv:1104.2314v1 [cond-mat.quant-gas] (2011).